UCSF

UC San Francisco Previously Published Works

Title

The H-Y Antigen in Embryonic Stem Cells Causes Rejection in Syngeneic Female Recipients

Authors

Hu, Xiaomeng
Kueppers, Simon T
Kooreman, Nigel G
et al.

The H-Y Antigen in Embryonic Stem Cells Causes Rejection in Syngeneic Female Recipients

Xiaomeng Hu,[1–3,*] Simon T. Kueppers,[1–3,*] Nigel G. Kooreman,[4–7,*] Alessia Gravina,[1,2]
Dong Wang,[1–3] Grigol Tediashvili,[1–3] Stephan Schlickeiser,[8,9] Marco Frentsch,[8]
Christos Nikolaou,[8] Andreas Thiel,[8] Sivan Marcus,[1] Sigrid Fuchs,[10] Joachim Velden,[11]
Hermann Reichenspurner,[2,3] Hans-Dieter Volk,[8,9] Tobias Deuse,[1,*] and Sonja Schrepfer[1–3,*]

Pluripotent stem cells are promising candidates for cell-based regenerative therapies. To avoid rejection of transplanted cells, several approaches are being pursued to reduce immunogenicity of the cells or modulate the recipient's immune response. These include gene editing to reduce the antigenicity of cell products, immunosuppression of the host, or using major histocompatibility complex-matched cells from cell banks. In this context, we have investigated the antigenicity of H-Y antigens, a class of minor histocompatibility antigens encoded by the Y chromosome, to assess whether the gender of the donor affects the cell's antigenicity. In a murine transplant model, we show that the H-Y antigen in undifferentiated embryonic stem cells (ESCs), as well as ESC-derived endothelial cells, provokes T- and B cell responses in female recipients.

Keywords: pluripotent stem cells, stem cell therapeutics, allograft, immunogenicity, Y-chromosome

Introduction

E VER SINCE THE first isolation of embryonic stem cells (ESCs) [1] from humans and the discovery of induced pluripotent stem cells (iPSCs) [2,3], the use of pluripotent stem cells (PSCs) for regenerative therapies is being explored for various types of diseases [4–8]. The transplantation of allogeneic ESC derivatives, however, triggers an immune response against major histocompatibility complex (MHC) antigens [9]. Unlike ESCs, iPSCs can be autologously derived, and the cell types generated from them could be accepted by the immune system upon reimplantation into the same host [10,11]. These findings have made iPSCs the focus of ''personalized regenerative medicine''.

For clinical applications, the situations in which cell products would be needed are likely to be time-sensitive, especially in acute onset diseases such as myocardial infarction and stroke. In this situation, the generation and upscaling of autologous stem cell products under good manufacturing practice conditions at the time of need are not feasible [12–14]. Furthermore, the quality of the cell product is dependent on the health status of the individual the cells were derived from. Earlier reports have shown that cells from diabetic donors have diminished regenerative capacity compared to healthy donors [15]. In addition, a higher donor age increases age-associated mutations that are passed over to iPSCs [16]. All of the abovementioned conditions for PSC quality have raised concerns about the feasibility of autologous iPSC therapies.

A way to circumvent these issues is by setting up cell banks to provide a haplotype match for the majority of the population. Calculations within the United Kingdom have shown that this can be achieved with 150 homozygous cell lines to provide a haplotype match for 93% of the population [17,18]. The costs for generating clinically usable PSC lines are estimated at around ~800,000 dollars per cell

¹Transplant and Stem Cell Immunobiology Lab, Department of Surgery, University of California, San Francisco, California, USA.
²Cardiovascular Research Center Hamburg (CVRC) and DZHK (German Center for Cardiovascular Research), Partner Site Hamburg/Kiel/Luebeck, Hamburg, Germany.
³University Heart & Vascular Center Hamburg, Hamburg, Germany.
⁴Stanford Cardiovascular Institute, ⁵Department of Medicine, and ⁶Institute for Stem Cell Biology and Regenerative Medicine, Stanford University, Stanford, California, USA.
⁷Department of Vascular Surgery, Leiden University Medical Center, Leiden, the Netherlands.
⁸BIH-Center for Regenerative Therapies (BCRT), Charité University Medicine and Berlin Institute of Health (BIH), Berlin, Germany.
⁹Institute of Medical Immunology, Charité Universitätsmedizin Berlin, Corporate Member of Freie Universität Berlin, Humboldt-Universität zu Berlin, BIH, Berlin, Germany.
¹⁰Institute of Human Genetics, University Medical Center Hamburg, Hamburg, Germany.
¹¹Evotec AG, Histopathology and In Vivo Pharmacology, Hamburg, Germany.
*These five authors contributed equally to this work.

line and would make the start-up costs for a stem cell bank higher than autologous PSC therapies [19]. However, larger stem cell banks could save millions of dollars in validation costs using screening strategies for pooled samples [20].

There has been an observation that male to female transplants of heart [21], liver [22], and kidney [23] show inferior outcomes and male recipients of female hematopoietic stem cell grafts are more likely to develop graft-versus-host disease (GVHD) [24,25]. Speculations about the existence of immunologically active minor histocompatibility antigens (miHAs) associated with the Y-chromosome have been raised.

Using ESCs generated by somatic cell nuclear transfer, our laboratory has recently shown that miHAs encoded by the mitochondrial DNA can cause immune rejection in otherwise genetically identical cells [26]. We now describe the immunogenicity of the H-Y miHA in a murine male-to-female ESC transplant setting. This H-Y miHA is preserved upon differentiation of ESCs and induces mainly T cell mediated responses. These findings suggest the use of female donor cells for allogeneic cell products in regenerative medicine.

Materials and Methods

Animals

Male and female BALB/c (BALB/cAnNCrl, H2^d) and SCID beige (CB17.Cg-PrkdcscidLystbg-J/Crl) were purchased from Charles River Laboratories (Sulzfeld, Germany) and received humane care in compliance with the Guide for the Principles of Laboratory Animals. Animal experiments were approved by the Hamburg ''Amt für Gesundheit und Verbraucherschutz''or the University of California San Francisco Institutional Animal Care and Use Committee and performed according to local and European Union (EU) guidelines and performed according to local and EU guidelines.

Mouse ESC culture and luc transduction

Male mouse ESCs (mESCs) were purchased from the Jackson Laboratory (Sacramento, CA; stock no. 000651) and grown on mouse embryonic fibroblasts (MEF) (Millipore, Burlington, MA) in knock out (KO) Dulbecco's modified Eagle's medium (DMEM) 10829 with 15% KO serum replacement, 1% glutamine, 1% minimum essential media-nonessential amino acid (MEM-NEAA) solution, 1% pen–strep (all Gibco), 0.2% beta-mercaptoethanol, and 100 U leukemia inhibitory factor (LIF) (both Millipore, Billerica, MA) to keep them pluripotent. Cells were maintained in 10 cm dishes, medium was changed daily, and the cells were passaged every 2–3 days using 0.05% trypsin-ethylenediaminetetraaceticacid (EDTA; Gibco). For the luciferase transduction, 1×10^5 mESCs were plated in one gelatin coated six well and incubated overnight at 37°C at 5% CO$_2$.

The next day, media was changed, and one vial of Fluc lentiviral particles expressing luciferase II gene under reengineered EF1a promotor (Gen Target, San Diego, CA) was added to 1.5 mL media. After 36 h, 1 mL of cell media was added. After further 24 h, complete media change was performed. After 2 days, luciferase expression was confirmed by adding D-luciferin (Promega, Madison, WI). Signals were quantified with Ami HT (Spectral Instruments Imaging, Tucson, AZ) in maximum photons per second per square centimeter per steradian.

Pluripotency analysis by reverse transcription-polymerase chain reaction

For reverse transcription-polymerase chain reaction (RT-PCR), RNA was extracted using the RNeasy Plus Mini Kit (Qiagen). Genomic DNA contamination was removed using the gDNA spin column. cDNA was generated using Applied Biosystems High-Capacity cDNA Reverse Transcription Kit. Gene-specific primers of the mouse induced pluripotent stem cells (miPSC) Characterization Kit (Applied Stemcell) were used to amplify target sequences. Actin was used as housekeeping gene, which encodes a cellular cytoskeleton protein. PCRs were performed on Mastercycler nexus (Eppendorf) and visualized on 2% agarose gels.

Cell transplantation

Before performing cell transplantations, mESCs were cultured in feeder-free conditions for one passage to avoid contamination with feeder cells. The cells were trypsinized and resuspended in 60 μL of sterile saline solution, followed by direct injection of the cell suspension into the right thigh muscle of recipient mice using a 26-gauge syringe.

Pluripotency testing in vivo

Two million miPSCs were injected intramuscular into the hind limb of immunodeficient severe combined immunodeficient (SCID)-beige mice, and teratoma development was observed within 28 days. Teratomas were recovered and fixed in 4% paraformaldehyde in phosphate-buffered saline (PBS), dehydrated, embedded in paraffin, and cut into sections of 5 μm thickness. For histopathology, sections were rehydrated and stained with hematoxylin and eosin (Carl Roth). Images were taken with an inverted light microscope.

Fluorescence in situ hybridization

Samples from pluripotency testing in vivo were cut into 5 μm thick sections. After deparaffinization, wax embedded tissue sections were pretreated with 0.01 M citrate buffer (Sigma; pH = 6.4) for 40 min at 90°C and incubated in Pepsin solution (Sigma) for 5 min at 37°C. Slides were rinsed in 70% ethanol before postfixed in 4% paraformaldehyde (PFA) solution for 2 min. Dehydrogenation was performed with ascending ethanol concentrations and were air dried at room temperature (RT) for 5 min. Y-Chromosome probe was diluted 1:5 in hybridization buffer and applied to the section, followed by denaturation at 80°C for 3 min. Slides were hybridized for 16 h at 37°C in a humid chamber. Posthybridization was performed, and slides were washed in 0.4 × saline-sodium citrate (SSC) buffer +0.3% Triton X-100 at 73°C for 2 min and 2 × SSC buffer +0.1% Triton X-100 at RT for 5 min. ProLong Gold antifade with 4,6-diamidino-2-phenylindole (DAPI) reagent (Invitrogen) was used to counterstain cell nuclei, and images were obtained with a SP5 laser confocal microscope (Leica).

Karyotyping

Cell harvest, slide preparation, and G-banded karyotyping were performed using standard cytogenetic protocols optimized for human pluripotent cells. Cells were arrested with 0.2 μg/mL colcemid for 2 h and trypsinized to detach the

cells from the plate. For hypotonic treatment, cells were placed in a hypotonic solution (0.075 M potassium chloride) for 15 min and afterward fixed in methanol/acetic acid (3:1). Metaphase chromosome spreads were heated for 15 min at 95°C, treated with 0.25% trypsin in Hanks' balanced salt solution (HBSS) (Gibco) for 6 s, and stained with Giemsa stain for 5 min. For karyotyping chromosomes of 15 cells were counted under the microscope, and karyograms from five captured images (CytoVision; Leica Biosystems) were prepared.

Enzyme-Linked ImmunoSpot

For unidirectional Enzyme-Linked ImmunoSpot (ELISPOT) assays, recipient splenocytes were isolated from fresh spleen 5 days after intramuscular injection of 1×10^6 male BALB/c mESCs and used as responder cells. mESCs were mitomycin inhibited and served as stimulator cells. 1×10^5 stimulator cells were incubated with 5×10^5 recipient responder splenocytes for 24 h according to the manufacturer's protocol (BD Biosciences, Heidelberg, Germany) using against interferon-gamma (IFN-γ, 551881; BD) and interleukin (IL)-4 (BD; 551878) antibody-coated 96-well filter bottom plates (Merck Millipore, Darmstadt, Germany; S2EM004M99).

Cytokine responses were detected using horseradish peroxidase Streptavidin (BD; 557630) and aminoethyl carbazole (AEC) Substrate (BD; 551951). Spot frequencies were automatically enumerated using an ELISPOT plate reader (AID GmbH, Strassberg, Germany) for scanning and analysis. Quadruplicates were performed in all assays.

Mixed lymphocyte reaction

For mixed lymphocyte reaction (MLR), 6×10^5 of the splenocytes isolated for the ELISPOT assays were stained using carboxyfluorescein succinimidyl ester (CFSE) (Molecular Probes, Eugene, OR; C34554) and then incubated with 6×10^6 mitomycin-inhibited mESCs for 3 days. Splenocytes that were unspecifically stimulated using phorbol 12-myristate 13-acetate (1 ng/mL; Sigma-Aldrich, Munich, Germany) and ionomycin (500 ng/mL; Sigma-Aldrich) were used as controls. The percentage of proliferated cells was assessed by flow cytometry (FACSCalibur; BD Biosciences).

Donor-specific antibodies

Sera from recipient mice were de-complemented by heating to 56°C for 30 min. Equal amounts of sera and donor ESC suspensions (5×10^6/mL) were incubated for 45 min at 4°C. Cells were labeled with fluorescence isothiocyanate-conjugated goat anti-mouse immunoglobulin M (IgM; BD Biosciences) and analyzed by flow cytometry (BD Biosciences).

CyTOF

Single-cell suspensions of the spleen were prepared by squeezing each organ through a 70 μm cell strainer. Erythrocytes were lysed with 2 mL ammonium-chloride-potassium (ACK) buffer lysing buffer (Thermo Fisher Scientific) for 4 min at RT. Single-cell suspensions were washed once, resuspended, and incubated for 5 min in 5 mL warm complete culture medium [Roswell Park Memorial Institute (RPMI) Medium containing 10% fetal bovine serum, 100 U/mL penicillin (Biochrom), 100 mg/mL streptomycin (Biochrom), and 50 mM 2-mercaptoethanol (Gibco) with 25 U/mL Pierce Universal Nuclease (Thermo Fisher)] to reduce viscosity and background from free DNA from any lysed cells as previously described [27–30]. A total of 3×10^6 cells per sample were stained in a 96 deep well plate with metal-conjugated antibodies in a final volume of 50 μL PBS for 30 min at RT. For the last 10 min of the reaction, 0.5 mM cisplatin (Fluidigm) was added to enable exclusion of dead cells. Cells were washed twice with flow cytometry buffer (0.1% bovine serum albumin, 2 mM EDTA in $1 \times$ PBS), and pellets were resuspended in 100 μL of 2% paraformaldehyde (in PBS) and incubated at 4°C overnight.

The following day, fixed cells were washed once with flow cytometry buffer and permeabilized using $1 \times$ saponin permeabilization buffer (eBiosciences) in PBS on ice for 1 h. Cells were washed once with flow cytometry buffer, and pellets were resuspended in 100 μL of nucleic acid Intercalator solution (12.5 nM Cell-ID Intercalator-Ir diluted in PBS) and then incubated at RT for 30 min. Cells were then washed twice with flow cytometry buffer, twice with ultrapure water, and adjusted to 0.5–0.7×10^6 cells/mL for acquisition. Cells were acquired on a CyTOF2 mass cytometer upgraded to Helios specifications (CyTOF2/Helios) (Fluidigm). The $0.1 \times$ EQ Four Element Calibration Beads (Fluidigm) were added to the samples for data normalization of the fetal calf serum (FCS) files using the CyTOF software. Tuning was performed each day before measurement following manufacturer's guidelines. Detailed method was previously described by Japp et al. [31].

Mass cytometry data analysis

Cytobank was used for initial manual gating and semi-automated SPADE-gating of predefined lineages as described previously [31–33]. All FCS files were transformed with Cytobank default arcsinh transformation (scale factor 5). Nucleated single cells were manually gated by DNA intercalators Ir191/Ir193, event length, and TER119 to remove debris, doublets, normalization beads, and erythrocytes. CisPt and CD45 were used to gate on viable leukocytes, which then served as input for SPADE clustering. Clustering was performed (downsampling percentage 10%, 50 target nodes) on lineage markers B220, CD11b, CD11c, CD19, CD3, CD4, CD8, F4/80, Ly6G, and TCRb. Based on the median marker expression levels, individual SPADE nodes were grouped and manually annotated into specific lymphocyte compartments, that is, B cells, CD4+ T cells, CD8+ T cells, or subsets of the innate compartment.

To resolve specific subpopulation, graph-based clustering [34] (using Rphenograph package) was conducted on pregated events within each compartment. The following differentiation or activation markers were selected for graph-based clustering: B220, CD138, CD19, CD38, CD40, CD44, CD62L, CD80, CD83, CD86, IgD, IgM, MHC-II, PD-L1, PD-L2 for B cells, CD25, CD38, CD44, CD62L, CD69, CD80, CD86, Ly6C, PD-L1 for CD4+, as well as CD8+, T cells, and B220, CD103, CD115, CD11b, CD11c, CD138, CD25, CD38, CD4, CD40, CD44, CD62L, CD8, CD80, CD83, CD86, F4/80, Ly6C, Ly6G, MHC-II, PD-L1, and PD-L2 for innate cells. Single clusters were merged and manually annotated into biologically relevant subsets with help of second-level hierarchical clustering on the same marker sets (Supplementary Fig. S1).

For statistical analysis of group differences in cell population abundances, that is, calculated as proportion of a given lineage, we fitted a generalized linear mixed-effects model for each cluster and population using the *lme4* package as described previously [35]. *P* values resulting from differential abundance testing were adjusted using the Benjamini–Hochberg procedure across all clusters and subpopulations. A false discovery rate-adjusted *P* value <0.05 was considered significant. All analyses were performed using R version 4.0.2, available free online at https://r-project.org

Medawar experiments

In accordance to the Medawar experiment, female neonatal mice (BALB/cAnNCrl; Charles River Laboratories) were immunized with 5×10^5 mitomycin-inhibited mESCs. In adulthood (after 6 weeks), the animals were reinjected with 1×10^6 mESCs (BALB/c Female re-inject), and unidirectional ELISPOT and MLR assays were performed to measure IFN-γ response and lymphocyte proliferation, as described above. Female BALB/c mice of the same age that were not immunized at birth served as controls (BALB/c Female Ctrl).

Teratoma formation assay

BALB/c male mESCs were plated on gelatin-coated flasks for one passage and subsequently for 30 min at 37°C to avoid feeder contamination. Cells were counted, and 1×10^5, 2.5×10^5, and 5×10^5 cells were transplanted intramuscularly into the indicated recipient mice using a 26 gauge needle.

Teratoma formation was observed and measured with a caliper (Mitutoyo, Neuss, Germany) on day 0, 1 and then every other day until day 29, subsequently every 10 days until day 60. Recipients with a teratoma size of >1,500mm^3 were euthanized.

In vivo lineage identification by immunofluorescence

Teratomas were recovered and fixed in 4% paraformaldehyde in PBS, dehydrated, embedded in paraffin, and cut into sections of 5 μm thickness. Immunofluorescence (IF) staining demonstrated differentiation into ectodermal, mesodermal, and endodermal cells using antibodies against brachyury (ab20680; Abcam), cytokeratin (ab192467; Abcam), and glial fibrillary acidic protein (GFAP) (GA5; Cell Signaling). For visualization, secondary antibodies conjugated with Alexa Fluor 555, 488, and 647 (all Invitrogen) were used, respectively. Cell nuclei were counterstained with DAPI, and imaging was performed with a Leica SP5 laser confocal microscope (Leica).

Derivation and characterization of mESC-derived endothelial cells

mESCs were plated on gelatin in 6-well plates and maintained in mESC media. After the cells reached 60% confluency, the differentiation was started and media was changed to RPMI-1640 containing 2% B-27 minus Insulin (both Gibco) and 5 μM CHIR-99021 (Selleckchem, Munich, Germany). On day 2, the media was changed to reduced media: RPMI-1640 containing 2% B-27 minus Insulin (both Gibco) and 2 μM CHIR-99021 (Selleckchem). From day 4 to 7, cells were exposed to RPMI-1640 media containing 2% B-27 minus Insulin plus 50 ng/mL mouse vascular endothelial growth factor (mVEGF; R&D Systems, Minneapolis, MN), 10 ng/mL mouse fibroblast growth factor basic (mFGFb; R&D Systems), 10 μM Y-27632 (Sigma-Aldrich, Saint Louis, MO), and 1 μM SB 431542 (Sigma-Aldrich). EC clusters were visible from day 7, and cells were maintained in endothelial cell growth medium (EGM)-2 SingleQuots media (Lonza) plus 10% fetal calf serum (FCS) heat-inactivated (hi) (Gibco), 25 ng/mL mVEGF, 2 ng/mL mFGFb, 10 μM Y-27632 (Sigma-Aldrich), and 1 μM SB 431542. The differentiation process was completed after 21 days and undifferentiated cells detached during the differentiation process. For purification, cells went through magnetic-activated cell sorting (MACS) purification according to the manufacturer's protocol using anti-CD15 mouse antibody-coated magnetic microbeads (Miltenyi, Auburn, CA) for negative selection.

The highly purified mESC-derived endothelial cells (mESC-ECs) in the flow-through were cultured in EGM-2 SingleQuots media plus supplements and 10% FCS hi. TrypLE was used for passaging the cells 1:3 every 3–4 days. Their phenotype was confirmed by IF for CD31 (ab28364; Abcam) and vascular endothelial (VE)-cadherin (sc-6458; Santa Cruz Biotechnology). Briefly, cells were fixed with 4% paraformaldehyde in PBS for 15 min. Cell membranes were permeabilized with Permeabilization solution (ASB-0102; Applied StemCell), followed by Blocking solution (ASB-0103; Applied StemCell) and incubation with the primary antibodies.

For visualization, cells were incubated with secondary antibody conjugated with AF488 or AF555 (Invitrogen). After nuclei staining with DAPI, images were obtained and analyzed with a Leica SP5 laser confocal microscope (Leica).

Tube formation assay was performed for mESC-EC characterization: 2.5×10^5 mESC-ECs were stained with 5 μM CFSE and 0.1 μg/mL Hoechst (both Thermo Fisher) for 10 min at RT and plated on 10 mg/mL undiluted matrigel (356231; Corning) in 24-well plates. After 48 h, tube formations were visualized by IF. For PCR analysis, RNA was isolated with the RNeasy Plus Mini Kit (Qiagen, Germantown, MD) according to the manufacturer's protocol. RT-PCR was performed to generate the cDNA (Applied Biosystems, Darmstadt, Germany). The following primers were used: VE cadherin forward: 5′-GGATGCAGAGGCTCACAGAG-3′, reverse: 5′-CTGGCGGTTCACGTTGGACT-3′.

Tube formation assay of mouse induced ECs

A 12-well plate was coated with 10 mg/mL Matrigel (356231; BD Biosciences, San Jose, CA) per well and incubated at RT for at least 30 min. The mESC-ECs were trypsinized using TrypLE Express, counted, and resuspended in 1 mL sterile PBS (Thermo Fisher) at a concentration of 5×10^5 cells, and 5 μM of CFSE (C34554; Thermo Fisher) was added. The cells were incubated at 37°C for 10 min, centrifuged, and ultimately seeded in the previously Matrigel-coated wells in EC medium.

After 45 h the cells were stained with 0.1 μg/mL Hoechst (Thermo Fisher) for 15 min at 37°C. Photos were taken with a Leica SP5 laser confocal microscope (Leica, Wetzlar, Germany).
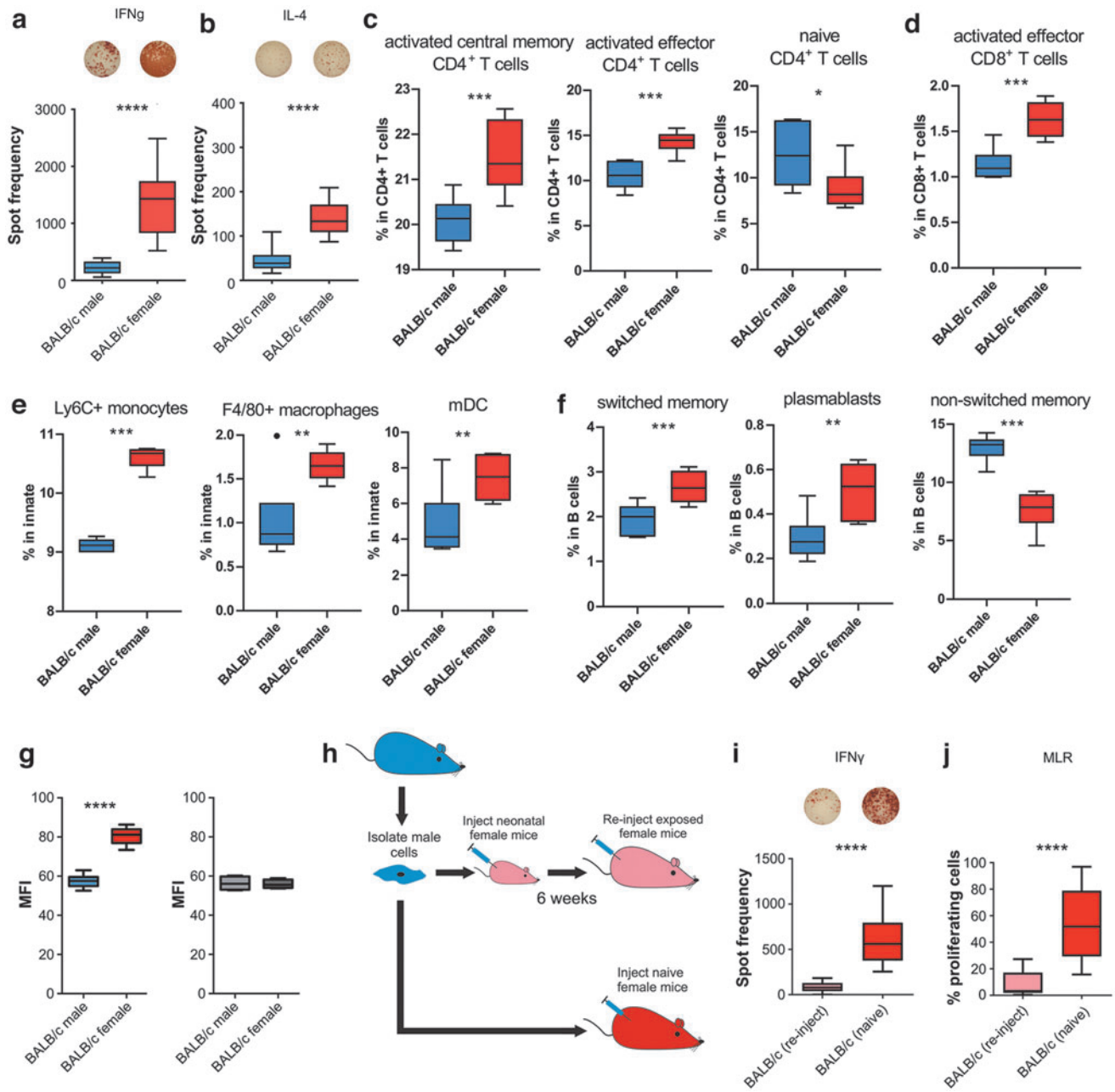
FIG. 1. Immune responses to mESCs carrying the Y chromosome. In ELISPOT assays, BALB/c female recipients ($n = 5$) showed higher spot frequencies than BALB/c male recipients ($n = 12$) for both **(a)** IFN-γ (Th1) and **(b)** IL-4 (Th2) activation. **(c–f)** Only box plots of immune cell subpopulations that show significant differences by the mass cytometry data analysis are shown. First, SPADE was used to gate four major immune populations (CD4^{+} T cells, CD8^{+} T cells, and innate and B cells) based on common lineage markers. Subsequently, clusters obtained by individual graph-based clustering of the major populations were merged and manually annotated into biologically comprehensible subpopulations and statistically compared between both mice groups (Supplementary Fig. S1). *$P < 0.05$, **$P < 0.01$, ***$P < 0.001$, ****$P < 0.0001$. **(g)** Mean fluorescence intensity of IgM binding to mESCs incubated with recipient serum after 5 days (mean ± SD, 5 female and 12 male animals per group, two-tailed Student's t-test), the background fluorescence in naive mice is shown in *gray* (mean ± SD, 3 animals per group, Student's t-test). **(h)** Diagram of Medawar experimental design comparing adult female mice with neonatal (tolerant state) exposure to male mESCs compared to naive female mice. **(i)**. In ELISPOT assays, BALB/c$_{reinject}$ ($n = 8$) showed a significantly lower IFN-γ response than BALB/c ($n = 12$). **(j)** In mixed lymphocyte reaction, BALB/c$_{reinject}$ ($n = 8$) showed significantly lower T cell than BALB/c ($n = 12$). All results ****$P < 0.0001$. mESC, mouse embryonic stem cell; SD, standard deviation; ELISPOT, Enzyme-Linked ImmunoSpot; IgM, immunoglobulin M; IFN-γ, interferon-gamma; IL, interleukin.

mESC-derived EC IF

mESC-ECs were stained for VE-cadherin (sc-6458; Santa Cruz Biotechnology) and CD31 (ab28364; Abcam, Cambridge, United Kingdom). The cells were plated on confocal dishes (P35GC-1.5-10-C; MatTek Corp., Ashland, MA) and fixed with 4% paraformaldehyde in PBS for 15 min. The permeabilization of the cell membranes was performed by applying the permeabilization solution (ASB-0102; Applied StemCell, Milpitas, CA) on the cells.

Subsequently, the permeabilized cells were blocked using a blocking solution (ASB- 0103; Applied StemCell) and incubated in the primary antibody (VE-cadherin or CD31, respectively) for 1 h at 37°C. The cells were then incubated for 1 h at 37°C with the secondary antibody conjugated with AF555 for VE-Cadherin and AF488 for CD31 (both Invitrogen). The nuclei were stained with DAPI and images obtained with a Leica SP5 laser confocal microscope (Leica, Wetzlar, Germany).

Bioluminescence imaging of ESC-ECs

Firefly luciferase overexpressing murine ECs were derived from BALB/c mESCs. Before injection, the cells were purified through MACS using CD15 microbeads (Miltenyi), and negative selection was performed. A 1:3 mixture of BD Matrigel High Concentration (354262; BD Biosciences) and sterile saline solution was prepared; 1×10^5 and 5×10^5, respectively, were resuspended in the mixture. Cells were injected subcutaneously in the right abdomen of male and female BALB/c mice with a 23 gauge needle.

The in vivo imaging of mESC-ECs was performed using the Ami HT platform (Spectral Instruments Imaging) on day 0, 1 and then every other day until day 29. Afterward they were imaged every 5 days until day 60.

D-Luciferin potassium salt (Biosynth AG, Staad, Switzerland) was diluted in PBS solution pH 7.4 (Thermo Fisher) and it was intraperitoneally injected (375 mg/kg) with an insulin needle to anesthetized mice (2% isoflurane).

Images were taken, and the signal was measured by applying a region of interest (measured in units of maximum photons per second per square centimeter per steradian) to each animal. The signal's maximum was recorded through the Aura imaging software (Spectral Instruments Imaging).

Statistics

In box blot graphs, the median is shown, the edges of the box are the 25th and 75th percentiles, and the whiskers extend to the most extreme data points. Intergroup differences were appropriately assessed by unpaired Student's t-test. ****$P < 0.0001$, ***$P < 0.001$, **$P < 0.01$, *$P < 0.05$.

Results

H-Y mismatched murine ESCs provoke T and B cell responses after transplantation

To assess the immunogenicity of the H-Y antigen, male or female BALB/c mice were injected with syngeneic male BALB/c ESCs, and 5 days later, their splenocytes were isolated and restimulated with the same male ESCs. Using the ELISPOT assay, both elevated IFN-γ and IL-4 immune responses were seen in female but not male recipients, indicating Th1 and Th2 immune response (Fig. 1a, b). For an immune system wide analysis of H-Y provoked immune responses splenocytes from female or male mice receiving male ESCs were analyzed by mass cytometry.

In line with the ELISPOT data, merged cluster of activated effector and central memory $CD4^+$ and $CD8^+$ T cells was significantly elevated in female mice treated with male ESCs (Fig. 1c, d). Signs of immune activation were also detectable by elevated proportion of inflammatory $Ly6C^+$ monocytes, macrophages, and myeloid-derived dendritic cells in female spleens (Fig. 1e). In addition, further indications of developing adaptive immunity provoked by H-Y ESCs were seen with an increase of plasmablast and activated cells with a switched-memory phenotype (Fig. 1f). Only female BALB/c recipients mounted a strong IgM antibody response against the male mESCs relative to baseline mean fluorescence intensity (MFI) (shown in gray) (Fig. 1g).

Acquired H-Y tolerance can be achieved during the neonatal developmental stage

To assess if the immunogenicity of the H-Y could be mitigated, we used the Medawar experimental setup to see if we could induce tolerance to the H-Y antigen (Fig. 1g). In brief, neonatal female BALB/c was injected at the neonatal stage with male BALB/c ESCs. After 6 weeks, the female mice were reinjected with the male ESCs and their splenocytes were isolated. An ELISPOT assay revealed significantly lower IFN-γ spot frequencies in these reinjected mice than in mice receiving their first ESC injection during adulthood (Fig. 1h).

Proliferation of the isolated splenocytes was assessed by an MLR assay and similarly revealed significantly less T cell proliferation in reinjected female mice (Fig. 1i). Again, our data show the immunogenicity of the H-Y antigen in syngeneic cell transplantation. However, tolerance toward this miHA can be induced during the neonatal phase of development.

FIG. 2. Survival of mESCs carrying the Y chromosome. **(a)** mESCs grown on a mouse feeder layer show colony formation typical of pluripotent stem cells. **(b)** G-banding shows a normal karyotype. **(c)** Polymerase chain reaction or pluripotency markers are positive in mESC, compared to the C57BL/6 fibroblast control. **(d)** Histology of mESC-sourced teratoma, formed in immunodeficient SCID/beige mice, reveals endoderm, mesoderm, and ectodermal lineage potential. **(e)** Fluorescence in situ hybridization from teratomas developed in animals from Fig. 2d demonstrates the presence of the H-Y chromosome in the donor cell population used in all in vivo assays. **(f)** Teratoma formation assays in male BALB/c mice reveals strong proliferative growth of ESCs with teratoma formation in 60% of mice receiving 1×10^5 male ESCs (*top panel*, $n = 6$) and in 100% of mice receiving 2.5×10^5 (*middle panel*, $n = 6$) and 5×10^5 (*bottom panel*, $n = 5$) male mESC. **(g)** In H-Y mismatched female BALB/c mice, teratoma formation is reduced to 0% of female mice receiving 1×10^5 male mESCs (*top panel*, $n = 6$), and 66.6% of mice receiving 2.5×10^5 male mESCs (*middle panel*), with only the group receiving 5×10^5 (*bottom panel*) male mESC reaching 100% teratoma formation ($n = 6$). **(h)** Positive immunostaining for cell mark-brachyury, cytokeratin, and GFAP, indicating the presence of cells from all three germ layers in teratomas developed in animals from Fig. 2f and g. GFAP, glial fibrillary acidic protein.
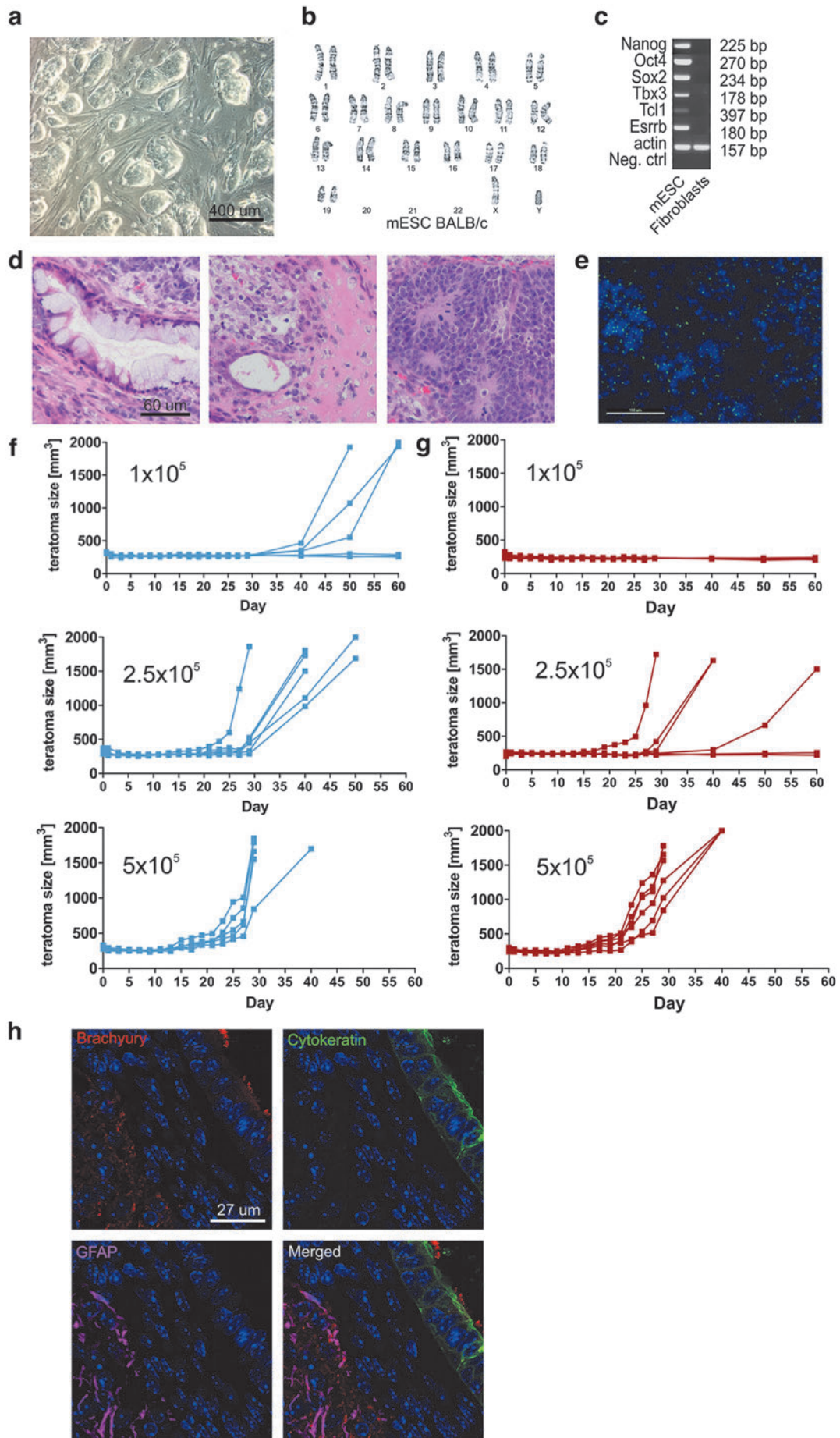
Limited survival of H-Y mismatched murine ESCs in syngeneic female mice

Pluripotency of ESCs was confirmed by PCR of in vitro cultures and in vivo teratoma development in SCID beige mice (Fig. 2a–d), and the presence of the Y chromosome after recovery of in vivo formed teratomas was demonstrated (Fig. 2e). Male and female BALB/c mice were then injected with syngeneic male ESCs, and survival of the transplanted cells was measured by teratoma formation over time.

Male-to-male ESC transplantation resulted in teratoma formation in 100% of the mice when 5×10^5 and 2.5×10^5 cells were injected (Fig. 2f) and 60% when 1×10^5 ESCs were injected. In contrast, while H-Y mismatched male-to-female transplants still achieved 100% teratoma formation with 5×10^5 ESCs with differentiating into all three germ layers (Fig. 2h), teratoma formation dropped to 66.6% with 2.5×10^5 cells and no teratomas were observed with only 1×10^5 cells (Fig. 2g). The impaired survival of H-Y antigen-carrying male cells in syngeneic female recipients demonstrates the relevance of this miHA as transplant antigen.

H-Y mismatched ESC-derived ECs show limited survival in female recipients

Next, the survival of ESC-derived ECs was assessed in vivo by bioluminescence imaging. Therefore, mESCs were differentiated into ECs (Fig. 3a) and subsequently transduced to express firefly luciferase (Fluc). ESC-EC grafts (5×10^5 cells) were injected into the thigh of synge-neic male or female recipients, and the survival was monitored. As expected, all male recipients allowed survival of syngeneic male ESC-ECs (Fig. 3b), whereas in female recipients the ESC-EC grafts got rejected (Fig. 3c).

Discussion

Immune responses against allogeneic human leukocyte antigen (HLA) are well recognized as a source of alloimmunity in organ transplantation [36,37], as well as cell transplantation [26,38–40]. The relevance of miHA in PSC alloimmunity was revealed with antigens encoded by the mitochondrial DNA [26]. We now describe that the H-Y antigen can induce T- and B cell immune responses after transplantation of PSCs or PSC-derived grafts. This antigenicity remains with differentiation of PSCs into ECs and supports the notion that immune barriers for PSC transplants include HLA and miHA mismatches.

First hints of Y-chromosomal antigenicity were described for skin grafts in the mid 1950s [41]. Subsequent studies found support for HLA class-I or class-II restricted presentation of such antigens, which can induce both cellular and humoral immune responses [42–49].

In allogeneic hematopoietic cell transplantation (HCT) donor and recipient HLA mismatching confers the highest proportional risk of GVHD [50]. However, Y-chromosome-encoded antigens have been identified that affect outcomes in sex-mismatched HCT [51].

Great hopes have been placed on human PSCs as novel therapeutic strategy for various diseases. Tissues or organs
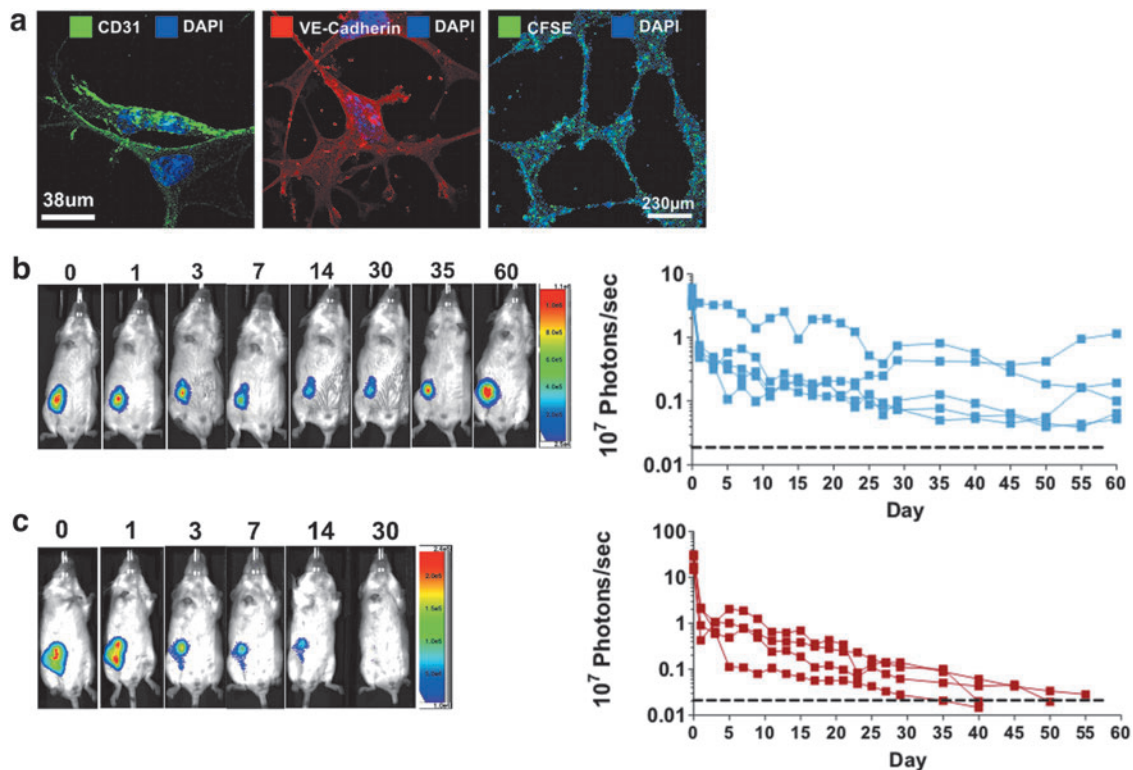

FIG. 3. H-Y immunogenicity in ESC-derived ECs. **(a)** Characterization of mESC-derived ECs showing CD31^{+} and VE cadherin^{+} staining, as well as the formation of tubes in a tube formation assay. **(b)** Tracking of luciferase labeled male mESC-ECs in vivo shows prolonged survival of cells after subcutaneous injection in male BALB/c recipients (*n* = 5/group), whereas **(c)** luciferase labeled male mESC-ECs were rejected within app. Fifty days in female BALB/c (*n* = 4/group). EC, endothelial cell. VE, vascular endothelial.

derived from PSCs could be the best solution to cure many different human diseases, especially those who do not respond to standard medication or drugs, such as neurodegenerative diseases, heart failure, or diabetes. The origin of PSCs is critical, and the idea of creating a bank of well-characterized PSCs has emerged [52]. Thus, understanding the effect of H-Y mismatches on the alloimmunity in PSC transplants is crucial and should not be underestimated.

Our data highlight the relevance of the H-Y antigen as miHA in PSC-derived cell transplantations and (although only demonstrated with one male cell line) are consistent with the conclusion that H-Y antigen expression by male PSCs does induce an immune response in female mice and does influence the ability of male PSCs to form teratomas. While this may not be relevant for allogeneic PSC approaches for which patients will be immunosuppressed due to HLA mismatches anyway, this phenomenon will be important for PSC strategies which aim to use HLA banks [17,18]. The goal is to avoid allogeneic rejection by matching the patient's HLA with the donor PSC to avoid or lower the need of immunosuppression. However, in this scenario miHAs (such as H-Y antigens) will get presented and will be recognized by the recipient's immune system [50,53,54]. Thus, antigenicity of H-Y should be considered when choosing for PSC banking.

Disclaimer

Acknowledgments

Author Disclosure Statement

Funding Information

Supplementary Material

Supplementary Figure S1

References

1. Thomson JA, J Itskovitz-Eldor, SS Shapiro, MA Waknitz, JJ Swiergiel, VS Marshall and JM Jones. 1998. Embryonic stem cell lines derived from human blastocysts. Science 282:1145–1147.
2. Takahashi K and S Yamanaka. 2006. Induction of pluripotent stem cells from mouse embryonic and adult fibroblast cultures by defined factors. Cell 126:663–676.
3. Takahashi K, K Tanabe, M Ohnuki, M Narita, T Ichisaka, K Tomoda and S Yamanaka. 2007. Induction of pluripotent stem cells from adult human fibroblasts by defined factors. Cell 131:861–872.
4. Caspi O, I Huber, I Kehat, M Habib, G Arbel, A Gepstein, L Yankelson, D Aronson, R Beyar and L Gepstein. 2007. Transplantation of human embryonic stem cell-derived cardiomyocytes improves myocardial performance in infarcted rat hearts. J Am Coll Cardiol 50:1884–1893.
5. Barberi T, P Klivenyi, NY Calingasan, H Lee, H Kawamata, K Loonam, AL Perrier, J Bruses, ME Rubio, et al. 2003. Neural subtype specification of fertilization and nuclear transfer embryonic stem cells and application in parkinsonian mice. Nat Biotechnol 21:1200–1207.
6. Soto-Gutierrez A, N Kobayashi, JD Rivas-Carrillo, N Navarro-Alvarez, D Zhao, T Okitsu, H Noguchi, H Basma, Y Tabata, et al. 2006. Reversal of mouse hepatic failure using an implanted liver-assist device containing ES cell-derived hepatocytes. Nat Biotechnol 24:1412–1419.
7. Pagliuca FW, JR Millman, M Gurtler, M Segel, A Van Dervort, JH Ryu, QP Peterson, D Greiner and DA Melton. 2014. Generation of functional human pancreatic beta cells in vitro. Cell 159:428–439.
8. Homma K, S Okamoto, M Mandai, N Gotoh, HK Rajasimha, YS Chang, S Chen, W Li, T Cogliati, A Swaroop and M Takahashi. 2013. Developing rods transplanted into the degenerating retina of Crx-knockout mice exhibit neural activity similar to native photoreceptors. Stem Cells 31:1149–1159.
9. Swijnenburg RJ, S Schrepfer, F Cao, JI Pearl, X Xie, AJ Connolly, RC Robbins and JC Wu. 2008. In vivo imaging of embryonic stem cells reveals patterns of survival and immune rejection following transplantation. Stem Cells Dev 17:1023–1029.
10. de Almeida PE, EH Meyer, NG Kooreman, S Diecke, D Dey, V Sanchez-Freire, S Hu, A Ebert, J Odegaard, et al. 2014. Transplanted terminally differentiated induced pluripotent stem cells are accepted by immune mechanisms similar to self-tolerance. Nat Commun 5:3903.
11. Zhao T, ZN Zhang, Z Rong and Y Xu. 2011. Immunogenicity of induced pluripotent stem cells. Nature 474:212–215.
12. Eschenhagen T and F Weinberger. 2019. Heart repair with myocytes. Circ Res 124:843–845.
13. Neofytou E, CG O'Brien, LA Couture and JC Wu. 2015. Hurdles to clinical translation of human induced pluripotent stem cells. J Clin Invest 125:2551–2557.
14. Shi Y, H Inoue, JC Wu and S Yamanaka. 2017. Induced pluripotent stem cell technology: a decade of progress. Nat Rev Drug Discov 16:115–130.
15. Gu M, NM Mordwinkin, NG Kooreman, J Lee, H Wu, S Hu, JM Churko, S Diecke, PW Burridge, et al. 2015. Pravastatin reverses obesity-induced dysfunction of induced pluripotent stem cell-derived endothelial cells via a nitric oxide-dependent mechanism. Eur Heart J 36:806–816.
16. Lo Sardo V, W Ferguson, GA Erikson, EJ Topol, KK Baldwin and A Torkamani. 2017. Influence of donor age on induced pluripotent stem cells. Nat Biotechnol 35:69–74.
17. Taylor CJ, EM Bolton, S Pocock, LD Sharples, RA Pedersen and JA Bradley. 2005. Banking on human embryonic

stem cells: estimating the number of donor cell lines needed for HLA matching. Lancet 366:2019–2025.

18. Taylor CJ, S Peacock, AN Chaudhry, JA Bradley and EM Bolton. 2012. Generating an iPSC bank for HLA-matched tissue transplantation based on known donor and recipient HLA types. Cell Stem Cell 11:147–152.

19. Bravery CA. 2015. Do human leukocyte antigen-typed cellular therapeutics based on induced pluripotent stem cells make commercial sense? Stem Cells Dev 24:1–10.

20. Devito L, A Petrova, C Miere, S Codognotto, N Blakely, A Lovatt, C Ogilvie, Y Khalaf and D Ilic. 2014. Cost-effective master cell bank validation of multiple clinical-grade human pluripotent stem cell lines from a single donor. Stem Cells Transl Med 3:1116–1124.

21. Khush KK, JT Kubo and M Desai. 2012. Influence of donor and recipient sex mismatch on heart transplant outcomes: analysis of the International Society for Heart and Lung Transplantation Registry. J Heart Lung Transplant 31:459–466.

22. Candinas D, BK Gunson, P Nightingale, S Hubscher, P McMaster and JM Neuberger. 1995. Sex mismatch as a risk factor for chronic rejection of liver allografts. Lancet 346:1117–1121.

23. Gratwohl A, B Dohler, M Stern and G Opelz. 2008. H-Y as a minor histocompatibility antigen in kidney transplantation: a retrospective cohort study. Lancet 372:49–53.

24. Carlens S, O Ringden, M Remberger, B Lonnqvist, H Hagglund, S Klaesson, J Mattsson, BM Svahn, J Winiarski, P Ljungman and J Aschan. 1998. Risk factors for chronic graft-versus-host disease after bone marrow transplantation: a retrospective single centre analysis. Bone Marrow Transplant 22:755–761.

25. Kollman C, CW Howe, C Anasetti, JH Antin, SM Davies, AH Filipovich, J Hegland, N Kamani, NA Kernan, et al. 2001. Donor characteristics as risk factors in recipients after transplantation of bone marrow from unrelated donors: the effect of donor age. Blood 98:2043–2051.

26. Deuse T, D Wang, M Stubbendorff, R Itagaki, A Grabosch, LC Greaves, M Alawi, A Grunewald, X Hu, et al. 2015. SCNT-derived ESCs with mismatched mitochondria trigger an immune response in allogeneic hosts. Cell Stem Cell 16:33–38.

27. Leipold MD and HT Maecker. 2012. Mass cytometry: protocol for daily tuning and running cell samples on a CyTOF mass cytometer. J Vis Exp 2012:e4398.

28. Leipold MD and HT Maecker. 2015. Phenotyping of live human PBMC using CyTOF mass cytometry. Bio Protoc 5:e1382.

29. Leipold MD, EW Newell and HT Maecker. 2015. Multiparameter phenotyping of human PBMCs using mass cytometry. Methods Mol Biol 1343:81–95.

30. Leipold MD, G Obermoser, C Fenwick, K Kleinstuber, N Rashidi, JP McNevin, AN Nau, LE Wagar, V Rozot, et al. 2018. Comparison of CyTOF assays across sites: results of a six-center pilot study. J Immunol Methods 453:37–43.

31. Japp AS, K Hoffmann, S Schlickeiser, R Glauben, C Nikolaou, HT Maecker, J Braun, N Matzmohr, B Sawitzki, et al. 2017. Wild immunology assessed by multidimensional mass cytometry. Cytometry A 91:85–95.

32. Kotecha N, PO Krutzik and JM Irish. 2010. Web-based analysis and publication of flow cytometry experiments. Curr Protoc Cytom Chapter 10:Unit10 7.

33. Qiu P, EF Simonds, SC Bendall, KD Gibbs, Jr., RV Bruggner, MD Linderman, K Sachs, GP Nolan and SK Plevritis. 2011. Extracting a cellular hierarchy from high-dimensional cytometry data with SPADE. Nat Biotechnol 29:886–891.

34. Levine JH, EF Simonds, SC Bendall, KL Davis, AD Amir el, MD Tadmor, O Litvin, HG Fienberg, A Jager, et al. 2015. Data-driven phenotypic dissection of AML reveals progenitor-like cells that correlate with prognosis. Cell 162:184–197.

35. Nowicka M, C Krieg, HL Crowell, LM Weber, FJ Hartmann, S Guglietta, B Becher, MP Levesque and MD Robinson. 2017. CyTOF workflow: differential discovery in high-throughput high-dimensional cytometry datasets. F1000Res 6:748.

36. Kissmeyer-Nielsen F, S Olsen, VP Petersen and O Fjeldborg. 1966. Hyperacute rejection of kidney allografts, associated with pre-existing humoral antibodies against donor cells. Lancet 2:662–665.

37. Patel R and PI Terasaki. 1969. Significance of the positive crossmatch test in kidney transplantation. N Engl J Med 280:735–739.

38. Lee SJ, J Klein, M Haagenson, LA Baxter-Lowe, DL Confer, M Eapen, M Fernandez-Vina, N Flomenberg, M Horowitz, et al. 2007. High-resolution donor-recipient HLA matching contributes to the success of unrelated donor marrow transplantation. Blood 110:4576–4583.

39. Petersdorf EW, TA Gooley, C Anasetti, PJ Martin, AG Smith, EM Mickelson, AE Woolfrey and JA Hansen. 1998. Optimizing outcome after unrelated marrow transplantation by comprehensive matching of HLA class I and II alleles in the donor and recipient. Blood 92:3515–3520.

40. Sasazuki T, T Juji, Y Morishima, N Kinukawa, H Kashiwabara, H Inoko, T Yoshida, A Kimura, T Akaza, et al. 1998. Effect of matching of class I HLA alleles on clinical outcome after transplantation of hematopoietic stem cells from an unrelated donor. Japan Marrow Donor Program. N Engl J Med 339:1177–1185.

41. Eichwald EJ and CR Silmser. 1955. Skin. Transplant Bull 2:148–149.

42. Miklos DB, HT Kim, KH Miller, L Guo, E Zorn, SJ Lee, EP Hochberg, CJ Wu, EP Alyea, et al. 2005. Antibody responses to H-Y minor histocompatibility antigens correlate with chronic graft-versus-host disease and disease remission. Blood 105:2973–2978.

43. Rosinski KV, N Fujii, JK Mito, KK Koo, SM Xuereb, O Sala-Torra, JS Gibbs, JP Radich, Y Akatsuka, et al. 2008. DDX3Y encodes a class I MHC-restricted H-Y antigen that is expressed in leukemic stem cells. Blood 111:4817–4826.

44. Spierings E, CJ Vermeulen, MH Vogt, LE Doerner, JH Falkenburg, T Mutis and E Goulmy. 2003. Identification of HLA class II-restricted H-Y-specific T-helper epitope evoking CD4+ T-helper cells in H-Y-mismatched transplantation. Lancet 362:610–615.

45. Vogt MH, RA de Paus, PJ Voogt, R Willemze and JH Falkenburg. 2000. DFFRY codes for a new human male-specific minor transplantation antigen involved in bone marrow graft rejection. Blood 95:1100–1105.

46. Vogt MH, E Goulmy, FM Kloosterboer, E Blokland, RA de Paus, R Willemze and JH Falkenburg. 2000. UTY gene codes for an HLA-B60-restricted human male-specific minor histocompatibility antigen involved in stem cell graft rejection: characterization of the critical polymorphic amino acid residues for T-cell recognition. Blood 96:3126–3132.

47. Vogt MH, JW van den Muijsenberg, E Goulmy, E Spierings, P Kluck, MG Kester, RA van Soest, JW Drijfhout, R Willemze and JH Falkenburg. 2002. The DBY gene codes for an HLA-DQ5-restricted human male-specific minor histocompatibility antigen involved in graft-versus-host disease. Blood 99:3027–3032.

48. Pennisi E. 1995. Long-sought H-Y antigen found. Science 269:1515–1516.

49. Warren EH, MA Gavin, E Simpson, P Chandler, DC Page, C Disteche, KA Stankey, PD Greenberg and SR Riddell. 2000. The human UTY gene encodes a novel HLA-B8-restricted H-Y antigen. J Immunol 164:2807–2814.

50. Wang W, H Huang, M Halagan, C Vierra-Green, M Heuer, JE Brelsford, M Haagenson, RH Scheuermann, A Telenti, et al. 2018. Chromosome Y-encoded antigens associate with acute graft-versus-host disease in sex-mismatched stem cell transplant. Blood Adv 2:2419–2429.

51. Popli R, B Sahaf, H Nakasone, JY Lee and DB Miklos. 2014. Clinical impact of H-Y alloimmunity. Immunol Res 58:249–258.

52. de Rham C and J Villard. 2014. Potential and limitation of HLA-based banking of human pluripotent stem cells for cell therapy. J Immunol Res 2014:518135.

53. Jameson-Lee M, V Koparde, P Griffith, AF Scalora, JK Sampson, H Khalid, NU Sheth, M Batalo, MG Serrano, et al. 2014. In silico derivation of HLA-specific alloreactivity potential from whole exome sequencing of stem-cell transplant donors and recipients: understanding the quantitative immunobiology of allogeneic transplantation. Front Immunol 5:529.

54. Abdul Razzaq B, A Scalora, VN Koparde, J Meier, M Mahmood, S Salman, M Jameson-Lee, MG Serrano, N Sheth, et al. 2016. Dynamical system modeling to simulate donor T cell response to whole exome sequencing-derived recipient peptides demonstrates different alloreactivity potential in HLA-matched and -mismatched donor-recipient pairs. Biol Blood Marrow Transplant 22:850–861.

Address correspondence to:
Sonja Schrepfer, MD, PhD
Transplant and Stem Cell Immunobiology (TSI) Lab
Department of Surgery
University of California
Medical Sciences S1207
513 Parnassus Avenue
San Francisco, CA 94143-2205
USA

E-mail: sonja.schrepfer@ucsf.edu